Civil Engineering and Architecture 10(6): 2410-2425, 2022 http://www.hrpub.org
DOI: 10.13189/cea.2022.100614

Effect of Axle Overloading on Pavement Structural Behaviour with Improved Clayey Subgrade Using PET Fibres

Arijit Kumar Banerji*, Pijush Topdar, Aloke Datta

Department of Civil Engineering, National Institute of Technology, West Bengal, India

Received June 3, 2022; Revised July 11, 2022; Accepted August 20, 2022

Cite This Paper in the Following Citation Styles

(a): *[1] Arijit Kumar Banerji, Pijush Topdar, Aloke Datta , "Effect of Axle Overloading on Pavement Structural Behaviour with Improved Clayey Subgrade Using PET Fibres," Civil Engineering and Architecture, Vol. 10, No. 6, pp. 2410-2425, 2022. DOI: 10.13189/cea.2022.100614*

(b): *Arijit Kumar Banerji, Pijush Topdar, Aloke Datta (2022). Effect of Axle Overloading on Pavement Structural Behaviour with Improved Clayey Subgrade Using PET Fibres. Civil Engineering and Architecture, 10(6), 2410-2425. DOI: 10.13189/cea.2022.100614.*

Copyright©2022 by authors, all rights reserved. Authors agree that this article remains permanently open access under the terms of the Creative Commons Attribution License 4.0 International License

Abstract Clayey subgrade soils are considered to have a lower bearing capacity, which may develop early pavement failure due to diverse axle loading. To avoid such failure issues, these soils must be treated prior to the beginning of the construction work. In the recent past, soil stabilization with plastic waste has become popular to reduce waste and improve soil behaviour. The current study aimed to use polyethylene terephthalate (PET) waste bottles to improve clayey subgrade soil for pavement construction. The PET fibre content varied between 1% and 5% by weight of the dry soil to investigate its influence on compaction, California bearing ratio (CBR), unconfined compressive strength (UCS), and tri-axial shear strength. The modified soil matrix with PET was further stabilized using Terrasil (0.1%) in order to improve the strength properties of the treated soil with ageing. Overall, the influence of the addition of the PET fibre on the structural behaviour of flexible pavement under diverse axle loading conditions was evaluated using Finite Element (FE) techniques. The pavement model is computationally implemented in ANSYS to study pavement structural behaviour in terms of surface deflection, vertical stress and strain on the subgrade layer, maximum shear strain in the bituminous layer, and tensile strain at the base of the bituminous layer under standard loading and overloading by 1.25 and 1.5 times. The test results indicated that the addition of PET fibres in subgrade soil significantly increases the CBR, UCS, and internal friction angle and decreases the compaction characteristics. The use of PET fibres in subgrade stabilization can result in a significant reduction in pavement thickness. FE analysis results compare pavement rutting performance and show that overloading reduces rutting life.

Keywords Clayey Subgrade Soil, Soil Stabilization, Polyethylene Terephthalate, Terrasil, ANSYS

1. Introduction

Road infrastructure has gradually increased, but it is found very often that pavement failure occurs at an early stage due to overloaded vehicles. The majority of users want to reduce transportation costs by overloading vehicles, although there are restrictions imposed by the regulatory authorities on the axle loads. The overloading phenomenon acts as an unexpected force, causing degradation in pavement performance even before the design life [1]. In most cases, roads are damaged due to heavy trucks, which usually have more than 0.80 MPa of tyre pressure along with overloading. Heavy vehicles, which account for about 15-20% of total traffic, are responsible for 60% of pavement damage and degradation [2]. Existing literature indicates that when a pavement is 5% overloaded, the

design life of the pavement is reduced from 15 years to 12.3 years. Similarly, with 10% and 20% overloading, the design life of a pavement is reduced to approximately 10 and 7 years, respectively [3].

According to Rys et al. [4], a 20% increase in overloaded vehicles results in a 50% decrease in mechanical performance. In addition to this, Assogba et al. [5] have identified the impact of overloaded low-speed traffic on pavement service life reduction and reported that low-speed vehicles increase the load duration on the surface. Moreover, the life cycle costs of overloaded vehicles are 30% higher than those of legally loaded vehicles [6]. Environmental and health impacts will develop adversely and intensify more rapidly in polynomial functions if the road life cycle is not reduced by a large amount [1]. It has also been shown that road regulation and road improvement can minimize pavement damage by 33-40 percent, or 7-8 years, during the course of a road's 20-year life span [7]. Despite the fact that overloading is a common practice in developing nations that violates legislation, less attention has been paid to the design components of structures that take this into consideration thus far.

To be able to carry the accelerated axle load, sufficient bearing capacity, as well as proper thickness and stiffness of the pavement layers, are required. Under the effect of heavily-loaded wheels, it is common for the subgrade to fail. The subgrade is considered the foundation of the pavement structure because of its ability to tolerate compressive stresses in the pavement. The use of local soil as a construction material may not always be acceptable due to a lack of suitable geotechnical properties [8]. Studies suggest that road construction built over clayey subgrade soils may experience lower bearing capacity, which may result in the failure of the highway pavements. Worldwide, the expansive clay soils are characterized as challenging and cause various challenges for engineers working on construction projects [9]. To avoid such problems, most studies have shown the use of soil stabilization techniques to improve the durability and serviceability of pavement structures. It allows the soil to adapt to traffic conditions and external variables on the construction site, like water level, rainfall, capillarity, soil permeability, evaporation, and drainage [10].

Soil stabilization generally discusses to the method of enhancing soil characteristics through the blending and mixing of various stabilizers [11]. In the recent past, soil stabilization with the use of waste materials like demolished construction materials, slurry, marble, glass powder, e-waste, plastic waste, and factory by-products has become popular. Studies have shown that utilizing waste plastic for stabilization of soil can enhance pavement foundations [13-17]. The most common type of plastic waste is plastic bottles made of polyethylene terephthalate (PET) [12]. PET is becoming one of the most common ways to package water around the world because it is lightweight and durable. Research findings have shown that adding waste plastic strips [13], low and high density polyethylene [14] pellets and strips, plastic strips mixed with brick dust [15], red mud and fly ash [16], lime and rice husk ash [17] as stabilizers increases the strength properties (California bearing ratio value, unconfined compressive strength and resilient modulus), and frictional resistance of subgrade soil. Besides, most research on the use of waste plastic in pavement has focused on the surfacing layer of flexible pavement [18]. Utilizing waste plastic can improve the bituminous physical properties and provide good adhesion properties. Thus, due to the lack of sufficient studies on the usage of plastic in subgrade layers, our knowledge of the influence of plastic waste on the geotechnical characteristics is similarly limited.

In recent years, there has been a growing interest in the application of additives based on nanotechnology to enhance various properties of the soil matrix. And as a commercially available soil stabilizer, Terrasil has been shown to improve geotechnical properties like unconfined compressive strength (UCS), permeability, compressibility, coefficient of consolidation, maximum dry density (MDD), and California bearing ratio value (CBR) [19,20].

Traffic loads on clayey subgrade soil can cause adverse pumping behaviour if they are sited in areas of high water tables, causing both construction and in-service stability problems [21]. This demands the use of a water-proof soil stabilization modifier to avoid these situations by preventing capillary rise and water ingress by retaining strength for a longer period of time. Plastic waste and a water proofing additive must be integrated to overcome this research gap. From a design standpoint, subgrade strength determines the pavement thickness, and the performance of pavement is largely dependent on the resilient modulus of subgrade. The results of the CBR test and empirical curves/design catalogues are used to calculate the pavement thickness and its composition. The CBR value has a major impact on the strength properties of the soil subgrade and is therefore a crucial parameter in identifying the soil characteristics relevant to pavement design and construction.

The failure life of pavement is predicted using an axle load repetition of 80 kN, with no consideration given to vehicle overloading. All the calculations related to pavement damage are based on the standard axle loading. In this context, the complex characteristics of pavement infrastructure necessitate the use of an analytical tool, and the application of Finite Element (FE) models provides the ideal solution. Most of the ongoing research in this area uses analytical models such as layered solutions [22] and numerical models like FEM [23, 24] to explore structural behaviour more minutely with the ability to incorporate realistic pavement material behaviour and boundary conditions. Such FE methods use two-dimensional or three dimensional models capable of considering static and dynamic loads, traffic loading frequencies, material parameters, and environmental factors.

In this paper, PET plastic waste was used as a

fibre-shaped reinforcement. In the laboratory, Modified Compaction, California Bearing Ratio, unconfined compressive strength, and shear strength tests were performed on subgrade soil stabilized with 0, 1, 2, 3, and 5% plastic waste. As mentioned, subgrade stabilization is a reliable method to reduce the resistance to deformation within the pavement where there is a high proportion of heavy traffic. The concern of overloading has received less attention when stabilized subgrades are implicated. Different combinations of axle overloading intensities with varying contact areas are explored to analyze the impact on lowering pavement critical strains from a rutting perspective. The ANSYS software was used to compare flexible pavement sections modelled with stabilized and un-stabilized subgrade soils. Nonlinearity is only assigned to the subgrade layer, and the other layers (bituminous surface, and granular base/sub-base) are assumed to behave in a linear elastic manner. The structural behaviour of the pavement is characterized in terms of surface deflection, vertical stress and strain on top of the subgrade, maximum shear strain in the bituminous layer, and tensile strain at the base of the bituminous layer under standard loading and overloading of 1.25 and 1.5 times. In addition, comparisons are made on the basis of pavement rutting life using the Indian Road Congress (IRC) 37:2018 code of practice.

2. Materials and Test Program

2.1. Materials

2.1.1. Subgrade Soil

The soil used in this study was collected from the Fuljhore area, Durgapur city (coordinates: 23.543148 N, 87.339667 E), West Bengal, India. The soil layer consists of firm to stiff, brownish to greyish clay. The soil is classified as a fine-grained type of CL (clays of low plasticity) as per the classification of the Unified System. The particle size distribution and physical properties of the local soil are shown in Table 1.

2.1.2. PET Plastic Waste Fibre

In this study, waste beverage bottles as polyethylene terephthalate (PET) were used as plastic fibre stabilizer, as shown in Figure 1. PET is a linear semi-crystalline thermoplastic polymer used in the process of making many types of plastic bottles. It is known for having a great variety of properties, like stability in shape and resistance to structural, temperature, and chemical reactions [25].

Figure 1. Waste Beverage Bottles (PET)

The plastic waste fibre that has been collected is cut into strips of 1.0 cm wide and 1.0 cm long. Four different percentages of PET (i.e. 1, 2, 3, and 5%) are mixed with soil. The dimension was chosen so that the pieces would be easy to blend and mix into the soil.

Table 1. Engineering properties of subgrade soil

Parameters (units)	Values
Particle size distribution	
Sand (%)	3
Clay (%)	42
Silt (%)	55
Physical Properties	
Liquid Limit (%)	44.2
Plastic Limit (%)	27.4
Plasticity Index (%)	16.8
Maximum Dry Density (g/cc)	1.75
Optimum moisture content (%)	19.2
CBR (Un-soaked) %	14.31
CBR (Soaked) %	4.7
UCS (kPa)	184
Cohesion (kPa)	33
Angle of Friction (degree)	27

2.1.3. Chemical Stabilizer: Terrasil

Terrasil, as shown in Figure 2 is a pale yellow-colored water soluble commercially available chemical additive (having a specific gravity of 1.01), used to stabilize geotechnical properties of soil subgrade. It uses nanotechnology to transform the water-absorbing hydroxyl groups into water-resistant alkyl Siloxane bonds, resulting in its hydrophobic nature. In the presence of soil, Terrasil reacts to develop a water-repellent layer, which makes the surface impervious to water. The chemical composition of Terrasil is Hydroxyalkyl-alkoxy- alkyl silyl (65-70%), Benzyl alcohol (25-27%), and Ethylene glycol (3-5%) [19].

Figure 2. Terrasil Chemical Stabilizing Agent

2.2. Test Program

Plastic strips with a 0.1 percent Terrasil [26] treatment percentage were investigated. Terrasil treated specimens were prepared by diluting Terrasil in water at OMC values. The spraying of Terrasil solution is done to simulate the top layer waterproofing in order to prevent water entry. Then the mould is put in a Terrasil solution for 1 minute to waterproof the bottom soil of the mould to simulate the stopping of bottom entry and capillary rise.

For characterizing compaction test, a modified proctor compaction test was performed to highlight increased densities for heavy loading conditions. This test was carried out as per IS 2720: (Part 8)-1983 [27] standards. 5 layers and 55 blows were used to compact the soil specimens with a 4.9 kg rammer. The compaction curve was established for each sample set using results of dry densities against corresponding moisture content. Then, the values for the Optimum Moisture Content (OMC) and the Maximum Dry Density (MDD) were found.

The CBR test method is used to evaluate the material's strength for the design of flexible pavement structures. The CBR test was performed in accordance with IS: 2720 (Part-16)-1987 [27]. The sample was loaded at constant rate of 1.25 mm/min till a 12.5 mm penetration was achieved through the plunger with a diameter of 50 mm. It has also been reported that treating soil with Terrasil changes soil characteristics over time and makes them hydrophobic [19,20]. Therefore, it was intended to study Terrasil's influence on strength parameters under curing conditions. In addition, it is reported in the literature that the stabilization effect of Terrasil on soil properties has a considerable effect after 7 days of curing. As such, in this study, different ageing intervals of 7 and 14 days were preferred. Initially, specimens were kept at a normal air temperature during the curing periods while using the open air curing technique. These samples were tested at different curing times, including no curing (4 days submerged), 7 days (7 days open air curing with 4 days submerged), and 14 days (14 days open air curing with 4 days submerged). The specimens were submerged/soaked in water for four days prior to testing to meet the pavement thickness/composition design standards specified by the CBR method (Figure 3).

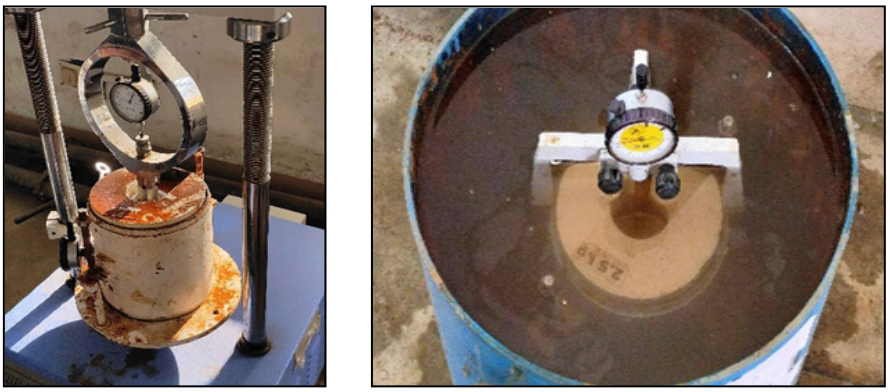

Figure 3. Experimental setup for soaked CBR Test

IS:2720 (Part 10)-1991 [29] was used to determine the soil's unconfined compressive strength. Three samples of 76.2 mm in height and 38.1 mm in diameter were prepared using their OMC. They were kept in sealed bags under optimum humidity conditions for seven days. Tri-axial test was carried out in this research in order to determine the influence of PET addition on shear tests in an undrained state. During the shearing phase, the drainage valve of the triaxial cell is opened to allow consolidation, and the valve is subsequently closed when confining pressure is applied. Pressures of 1.0 and 1.5 kg/cm^2 were applied till the sample failed. This test was performed in accordance with ASTM D4767-11 [30] under undrained conditions and the highest applied stress at failure was measured. At OMC, the soil sample was then compacted in a split mould with a height of 76.2 mm and a diameter of 38.1 mm. The deviator stress, strain, and stress ratio were determined, and the Mohr's circle was established for each sample set to evaluate the shear parameters (cohesion and friction angle).

3. Flexible Pavement Structural Configuration

ANSYS 2020R1 software was used to create the three-dimensional (3-D) finite element pavement model. This FE model was used to assess the effectiveness of flexible pavement created with PET fibre and Terrasil stabilized soil structure. The analyzed pavement section is composed of a bituminous layer, an aggregate granular base, a granular sub-base, and a soil subgrade layer. In the top structural layer (surface course), two layers are separated by the wearing course on top and the binder course on the bottom.

3.1. Pavement Material Properties

The modulus of elasticity, the poisson's ratio, and the density of the pavement material are used to characterize the layer in modelling. The material description of the surface course and granular base-sub base layers is adopted from IRC: 37-2018 [31] specifications. Although the viscoelastic material behaviour realistically simulates the bituminous layer of a pavement structure, it requires complex laboratory facilities to identify its parameters, as well as the numerical analysis requires more computer time [32]. For simplification, the bituminous layer is represented as linear elastic. This assumption is also used by other researchers [32,36,37]. The values of the surface course modulus are dependent on an annual mean temperature of 40°C. for the pavement, with BC for VG40 bitumen [31].

Granular base and sub-base layer material behaviour are also considered as linear elastic to have a clear comparison of the pavement behaviour in investigating the effect of using improved subgrade. To calculate the granular layer's (M_{Rgran}) resilient modulus equation (1) is required, which is based on the value of the subgrade resilient modulus ($M_{Rsubgrade}$). The correlation formula recommended by IRC 37-2018 is adopted to determine the subgrade (M_{RS}) resilient modulus as mentioned using equation (2).

The subgrade layer was assumed to be non-linear and simulated using the Mohr–Coulomb plasticity model in ANSYS. To accomplish this, in addition to the linear elastic parameters (i.e. elastic modulus and Poisson's ratio), the cohesion parameter (c), the angle of internal friction parameter (φ), and the dilation angle parameter (ψ) are incorporated into the model. Many researchers have been using the Mohr–Coulomb plasticity model because of its simplicity and its potential to provide realistic solutions to various geotechnical engineering challenges [38]. The inputs for material properties and dimensions for FE modelling are listed in Table 2, and the subgrade plasticity model parameters are considered from tri-axial shear test results as reported in Table 4.

$$M_{Rgran} = 0.2 \times \text{thickness of granular layer}^{0.45} \times \times M_{Rsubgrade} \quad (1)$$

$$M_{RS} = 10 \times CBR \text{ (for CBR<5); and}$$

$$M_{RS} = 17.6 \times CBR^{0.64} \text{ (for CBR>5)} \quad (2)$$

Table 2. Pavement material properties and dimensions

Layers and Thickness	Material Property	Values
Wearing Course (BC) 40 mm	Elastic modulus (MPa)	2000
	Density (kg/m^3)	2400
	Poisson's ratio	0.35
Binder Course (DBM) 140 mm and 125 mm	Elastic modulus (MPa)	2400
	Density (kg/m^3)	2400
	Poisson's ratio	0.35
Granular layer (Base and subbase) 250 and 200 mm	Elastic modulus (MPa)	156 & 192
	Density (kg/m^3)	1800
	Poisson's ratio	0.35
Subgrade (Infinite)	Elastic modulus (MPa)	47 & 62
	Density (kg/m^3)	1900
	Poisson's ratio	0.35

3.2. Finite Element Model Configuration

The FE mesh employed and the modelled pavement geometry shown in Figure 4 had completely continuous (perfectly bonded) interface layers. In the finite element simulation, the quarter model pavement section was taken into account with the application of half axle load. The ANSYS 3-D FE model was built using an 8-node linear brick element, SOLID45. The finite domain size of a quarter-model pavement block is 1.3 m in length and 1.5 m in width, with a 3.16 m overall depth. Previously, a similar

assumption was satisfactorily used for the analysis of a flexible pavement system using FE modelling [24]. Table 2 lists the pavement layer thicknesses selected according to the 50 million standard axle traffic design catalogues for CBR 5 and 7%. Two types of pavement models, denoted as Pavement 1 and 2, have been simulated considering 5% CBR (un-stabilized) and 7% CBR (stabilized) values.

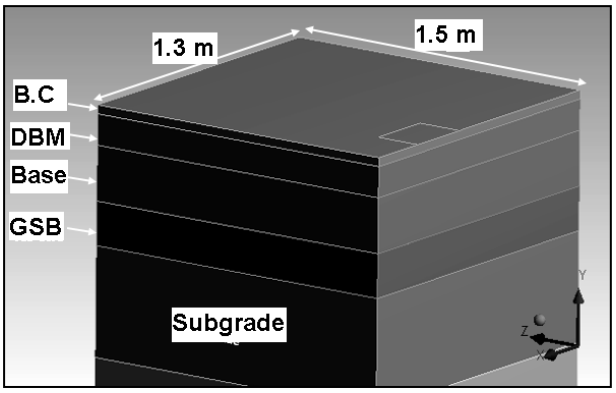

Figure 4. Pavement Model considered in the FE Analysis

3.3. Loading and Boundary Conditions

In the case of overloading, wheel load imposes the most stress when it is directly on top of the pavement surface, whereas it exerts the least stress when it is distant from the loading location. As a result of this, it is realistic to assume that the loading waveform either has a sinusoidal or a triangular shape, with stress durations depending on the speed of the vehicle as well as the depth of the pavement section [32]. In this study, a triangular wave with 40, 50, and 60 kN peak load is implemented; see Figure 5. The loading waveform has a duration of 0.1 s. The pressure exerted by the tyre on the surface was considered to be 560 kPa and distributed equally over the loading area during the simulation. The majority of studies make the assumption that the tyre contact area is circular or rectangular. In a finite element analysis of pavement structure, the pattern of the tyre impression was optimized to have an equivalent rectangular area of contact with the pavement surface [22,24]. According to Huang's recommendation, the tyre contact patch area is considered as a geometry of two semicircles and a rectangle, which is transformed to a rectangular area of 0.5227 L^2 having a width of 0.6 times the length. Using the recommendation, the following dimensions are obtained considering the standard axle and overloading cases, as mentioned in Table 3.

Table 3. Tyre contact area dimensions

Axle Loading Cases	Case 1: Standard Axle Load	Case 2: Overloading Factor 1.25	Case 3: Overloading Factor 1.5
Load (kN): Dual wheels	80	100	120
Load (kN): Single wheels	40	50	60
Length (mm)	320	360	390
Width (mm)	220	250	270

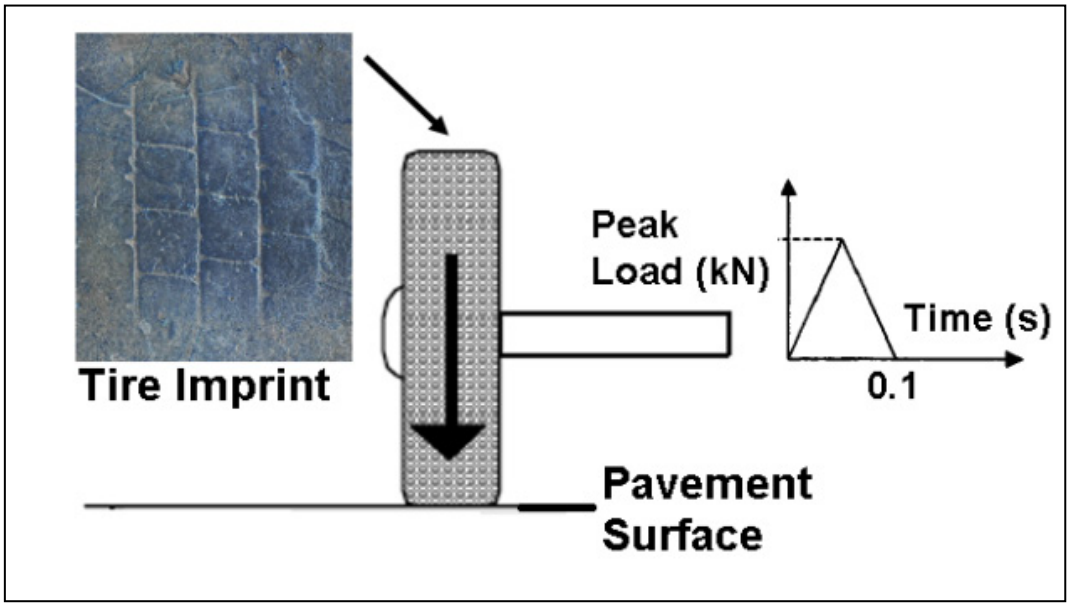

Figure 5. Tire imprint and loading-time function

To apply the overloaded traffic situation on the road surface, hypothesized conditions are assumed, in which the 1.25 and 1.5 overloading factors are considered for the single axle truck. Axle spacing for a single axle was considered as 1.2m. With a resemblance to the field boundary condition, orthogonal displacements to the plane of symmetry between the tyres are restrained on the side faces of the model. Fixed support has been considered at the bottom face of the model, representing the sub-grade layer. Roller support has outlined the vertical faces away from the wheels. Similar boundary assumptions have also been adopted in the literature [23,24].

3.4. Model Verification

A previously validated three-dimensional FE model [24] was utilized to calculate pavement responses in this study. To confirm the reliability of the pavement model, linear elastic responses were obtained using 3D FE analysis. A refined mesh was used directly under the wheel load, and a medium mesh was used away from the loading path to reduce computation time. For the objective of convergence study, the element size of 5 mm to 0.05 mm has been adjusted at and near the tyre impression. The element size of 0.05 mm was chosen depending on the mesh convergence analysis. Result verification was done by comparing linear elastic solutions observed at 600 mm depth. The tyre impression is 198 mm by 144 mm, equivalent to 700 kPa and 20 kN. The elastic moduli of 1800 MPa (asphalt layer), 1725 MPa (granular base), 55.20 MPa (subbase), 96.6 MPa (calcareous clay sand), and 72.45 MPa (clayey soil) have been considered. Poisson's ratio for top asphalt layers and underneath layers has been taken as 0.3 and 0.35, respectively. Deflection vs distance from the point of load application is plotted in Figure 6 for distances of 0, 200, 250, 300, 500, 600, 900, 1200, and 1500 mm. It can be seen that the outcomes from the analysis are consistent with the results from Hadi and Bodhinayake's previous research [24]. Deflection results are having (0.32-0.34) a variance of 6%, and the comparison between the values and the trend of deflection matches well.

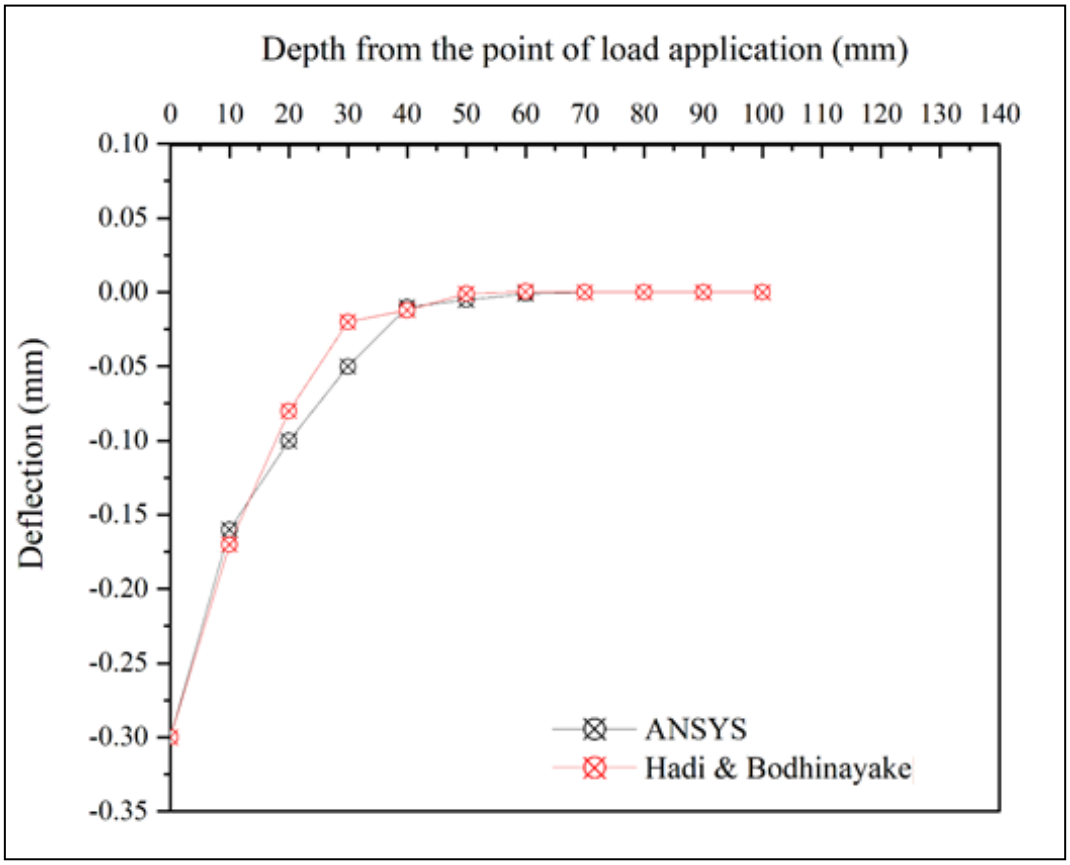

Figure 6. Comparison of the deflections obtained at 600 mm depth in the present FE model and Literature [24]

4. Results and Discussion

4.1. Effect of PET on Compaction Characteristics

The potential of PET fibres for the enhancement of geotechnical properties is being investigated by compaction properties. The findings of the OMC and corresponding MDD values are presented in Figure 7 for the unstabilized and stabilized soil with PET at different content ratios. The MDD value of the soil sample was 1.75 gm/cc and the OMC was 19.2% without plastic additives. Compared with un-stabilized specimen, the compaction characteristic values decrease for the stabilized soil for the range of PET ratios examined. When fibre content increases, both of these properties are reduced. The MDD reduction value for PET is from 1.72 g/cc for 1% PET content to 1.67% for 5% PET content. The maximum reduction of 20% in OMC was obtained at 5% fibre content. Similar findings were observed by Amena [13], Abukhettala and Fall [14], Amena [15] and Bala [16]. They showed that the value of OMC and MDD decreases as the percentage of the plastic is increased. This is because plastic materials are not water absorbing materials, unlike clay soils, which have a strong attraction to moisture caused by the surface tension of the material.

4.2. Effect of PET on Strength Parameters and Pavement Thickness

The effectiveness of PET fibres with chemical stabilizer in improving subgrade strength has been investigated in this work, with consideration of CBR values. Table 4 shows the 4-day soaked CBR values. The CBR value after soaking was 4.7% for unstabilized soil. According to the results, the clayey soil was significantly strengthened by the addition of PET and Terrasil. CBR has increased by 53% from 4.7 to 7.2 due to the increase in the fibre concentration ratio. Adding plastic fibre has been shown to improve the CBR value by increasing resistance to penetration due to soil-fibre interactions. Under aged conditions, the treated soil's strength improved significantly. This is because Terrasil has a stabilizing effect on the soil, which makes the soil particles bond together. The CBR value at 2.5 mm penetration was observed to be higher than at 5.0 mm for un-stabilized and stabilized cases evaluated in this investigation. Figure 8 represents the change in CBR caused by different curing days (0, 7, and 14). The samples are examined at various curing periods to see how curing affects soil mixed Terrasil responses.

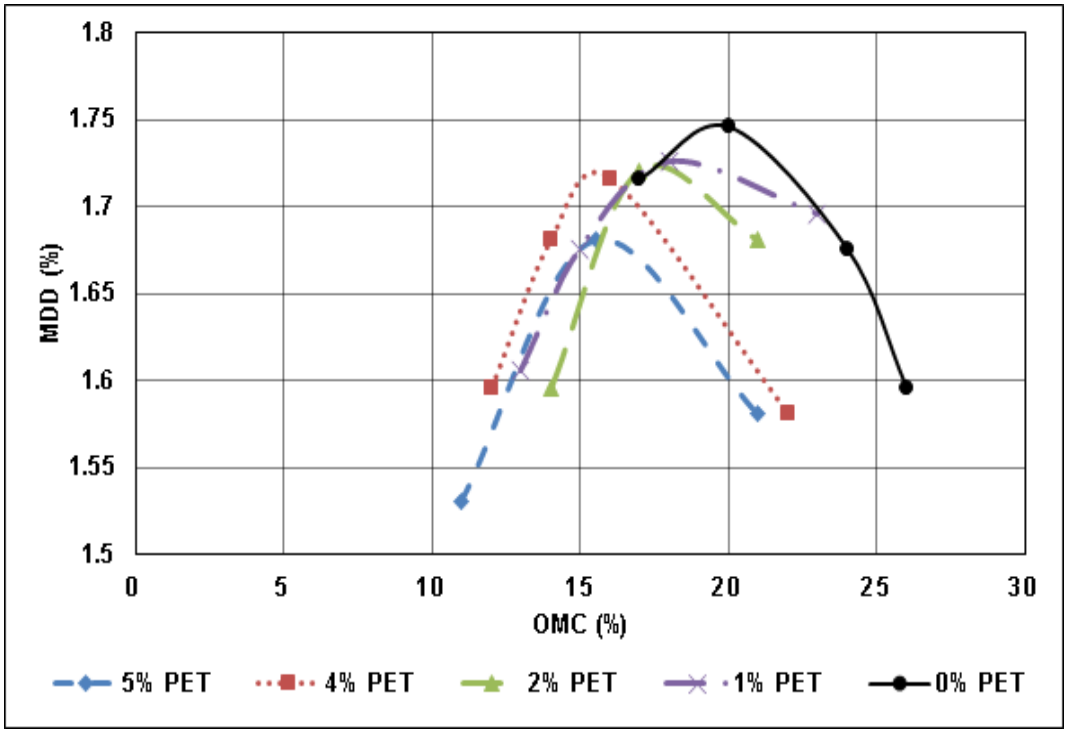

Figure 7. Modified Proctor test results for different PET contents

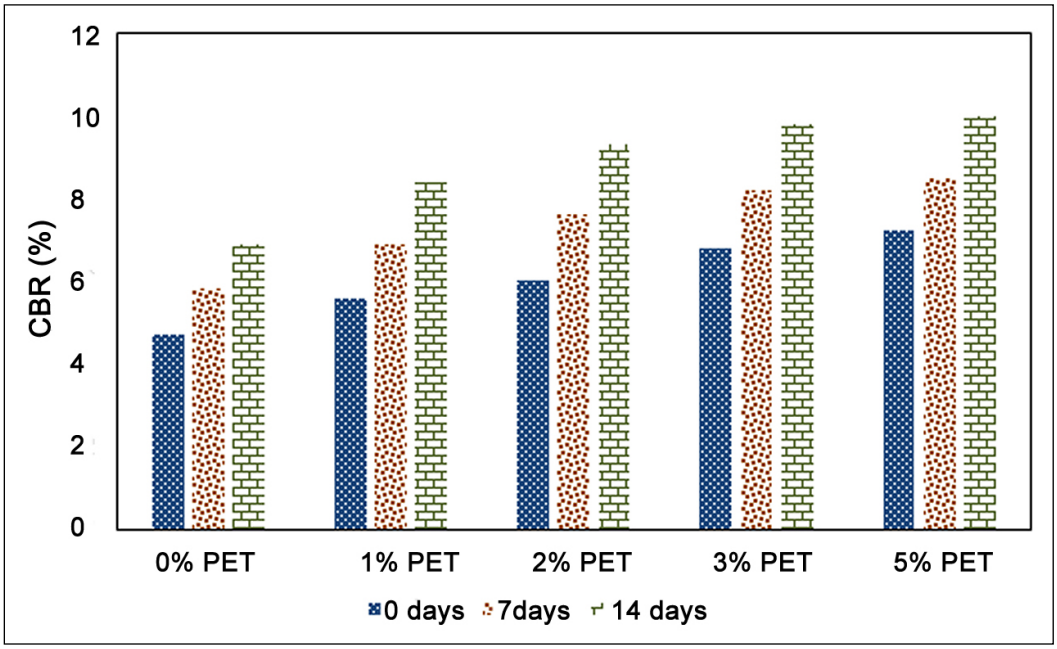

Figure 8. CBR values based on different curing days

Table 4. Effect of PET on strength and shear parameters

PET Fibre Content (%)	4 days Soaked CBR (%)	UCS (%)	Cohesion (kPa)	Internal friction angle (°)
0	4.7	184	33	27
1	5.6 (+19%)	238 (+29%)	41 (+24%)	29 (+7%)
2	6.0 (+27%)	251 (+36%)	43 (+30%)	33 (+22%)
3	6.8 (+44%)	240 (+30%)	46 (+40%)	38 (+40%)
5	7.2 (+53%)	232 (+26%)	45 (+36%)	39 (+44%)

*The values in parentheses indicate percentage change from case 0% PET to 1,2,3, and 5%.

In terms of quantitative strength, treated soil is approximately 1.5 times more resilient than untreated local soil, which is in good agreement with past researchers. This improvement is likely as a result of the stabilizer reaction with the soil mass, as it maintains dry specimens in wet environments. The improved strength at 14 days of the curing is about 1.3 to 1.7 times the CBR at standard curing. In accordance with the findings of this study, curing the Terrasil-treated soil is necessary for increasing its characteristics when used in field applications. As per IRC 37 design methods, pavement thickness is dependent on the soaked subgrade soil CBR values, and this increment in CBR values shows a significant impact on pavement thicknesses and road pavement construction costs. The improvement in CBR value causes a reduction in the pavement thickness (630mm to 615mm). Predominantly, the difference is in the DBM layer from 140mm to 125mm, with a percentage difference of around 12%. This reduction in the layer thickness also results in a construction cost reduction for the pavement. On the other hand, considering the CBR result in evaluating subgrade moduli, the resilient modulus values of subgrade increased by 30% (48 MPa to 62MPa).

According to Table 4, the addition of PET fibre considerably improved the stabilized strength properties compared to local strength parameters. While UCS increases as fibre content increases, there is an optimum increase in UCS value up to 2% PET, then the percentage increase flattens and maintains the same strength as fibre content increases. Thus the fibre has a significant role in increasing the UCS of the clayey soil by allowing it to withstand greater loads.

The cohesion and angle of internal friction values in the shear tests performed on the locally available soil have shown comparatively lower values. Soils treated with Terrasil and PET have improved strength parameters, as they show good increase in cohesion and angle of internal friction. The increased friction between clay particles and fibres is a result of increased soil-fiber contact as PET fibre content increases [33]. There seems to be a high degree of cohesion between soil particles because it is

difficult for soil particles to move around fibres. To explore the wide effect of PET, subgrade nonlinearity was simulated by the Mohr–Coulomb plasticity model in ANSYS. The c, φ and ψ values are determined from tri-axial shear testing results. These values are 33kPa, 27° and 0° for unstabilized soil, and 45kPa, 39° and 9°, respectively, for stabilized soil.

4.3. Effect of Overloading on Pavement Deflection

The analysis incorporates overloading situations as well as improved subgrade properties in order to better understand the relationship between these two parameters and surface deflection. Figure 8 represents a comparative result of the variations in surface deflection values in Pavements 1 and 2 at different loading cases. This figure shows that the increment of overloading greatly influences the trend of the vertical deflection curve in relation to the distance from the loading edge of the pavement. In Figure 9, the highest deflection of 0.524 mm is noted when an overloading factor of 1.5 is applied to it. Compared with the 1.25 and 1.5 overloading factors on conventional un-stabilized pavement, the resistance to deformations is more prominent under overloading, with a rise from 15% to 30%.

This indicates that when the percentage of axle load increases, the surface deflection value tends to increase. An additional comparison of the variations in deflection between Pavement models 1 and 2 is shown in parenthesis (Tables 5 and 6) at the bottom of the binder course and at the top of the subgrade. For the higher overloading factor, it can be stated that the case 3 model has a higher sensitivity to material properties on the performance of deflection on top of the subgrade. Overall, the improved subgrade pavement model shows more resistance to deformations (2.6 percent) under different overload factors.

4.4. Effect of overloading on Pavement Structural Responses

Structural response parameters including fatigue strain as maximum horizontal strain under the bituminous layer, maximum shear strain in the bituminous layer, and rutting strain as maximum vertical strain on the top of the subgrade have been investigated in the present study. In order to perform the numerical simulations, a total of six models have been developed and evaluated, as shown in Tables 5 and 6. Figure 10 represents the distribution of tensile and shears strain in the bituminous layer under overloading criteria for an un-stabilized and stabilized pavement model, respectively. It can be seen in Figure 10 (i) that the strain rate increases as the axle load is increased, and that the strains on the top section of the bituminous layer are compressive in the bottom section. It can also be seen that, for both pavements 1 and 2, the compressive strain changes to be tensile.

Compared with the overloading factor of 1.25 and 1.5 on conventional un-stabilized pavement, maximum tensile strain under the bituminous layer rises from 25 to 32%. From Tables 5 and 6, it has also been noticed that the maximum difference in the case of tensile strain is 33%, while it is up to 9% in the case of shear strain. It shows the subgrade performance has a very minor effect on the fatigue strain transferred to the bottom of the bituminous layer. The reason could be that improved subgrade characteristics affect the fatigue of pavements with reduced DBM layer thickness in Pavement 2.

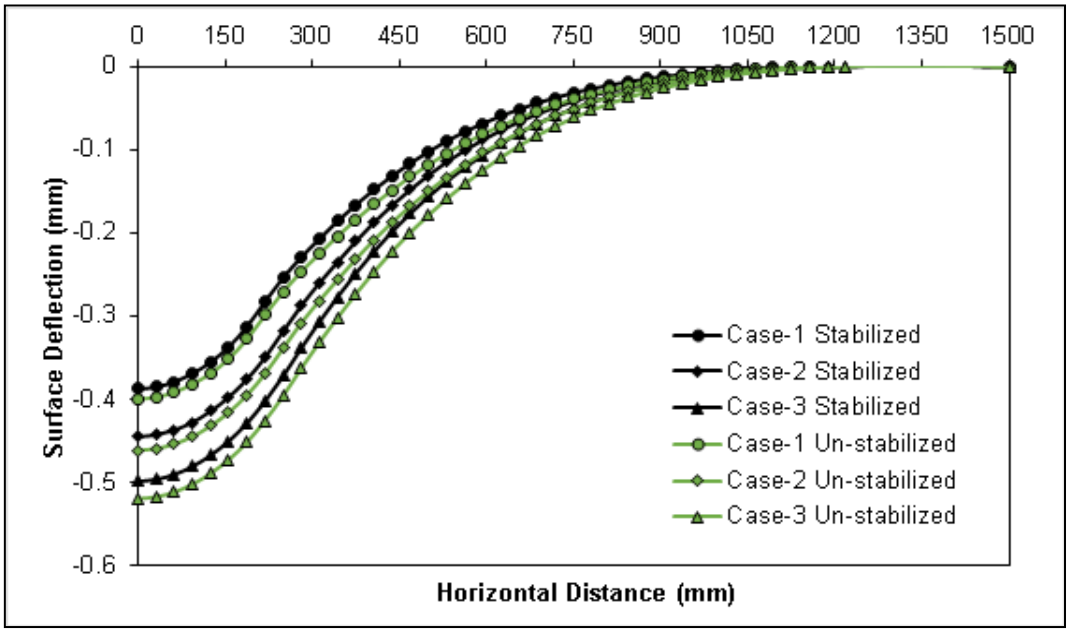

Figure 9. Comparison of the surface deflection in un-stabilized and stabilized models

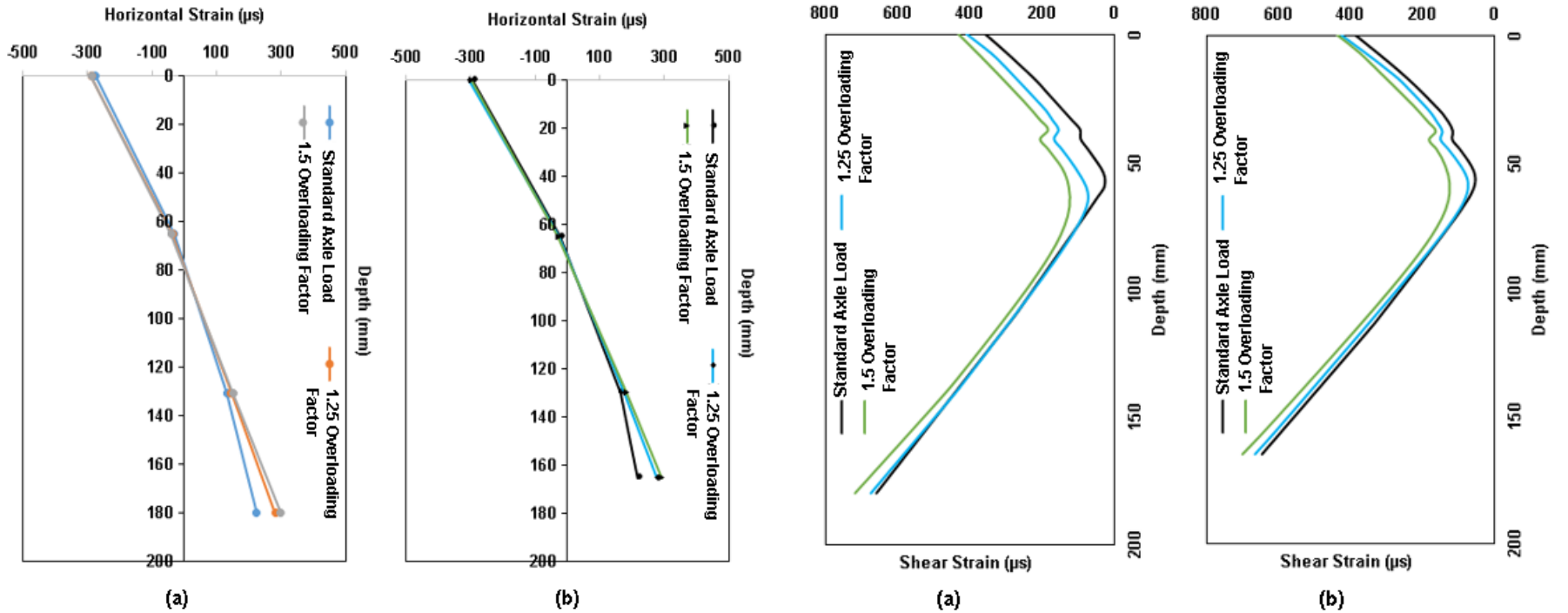

Figure 10. (i) Variation in the horizontal fatigue strain with depth (ii) Variation in the shear strain with depth in (a) Un-stabilized and (b) Stabilized models

As shown in Figure 10 (ii), the shear strain increases with depth until it reaches its maximum, at which point it decreases. Pavement 1 and 2 have maximum shear strain increases of 3% (659-674 micro strain and 646-665 micro strain) and 9% (659-718 micro strain and 646-704 micro strain) for 1.25 and 1.5 overloading factors. In pavements 1 and 2, tensile strain is much less than shear strain, indicating that shear deformation is the predominant mode of deformation in the bituminous layer.

Table 5. Comparison of pavement responses calculated from FE simulated Un-stabilized local subgrade model

Pavement responses	Case 1: Standard Axle Loading	Case 2: 1.25 Overloading Factor	Case 3: 1.5 Overloading Factor
δ Surface (mm)	-0.402	-0.463 (+15)	-0.524 (+30)
δ bottom of bituminous layer (mm)	-0.373	-0.441 (+18)	-0.499 (+34)
δ top of subgrade (mm)	-0.098	-0.118 (+20)	-0.138 (+40)
Maximum tensile strain under bituminous layer (microstrains)	225	282 (+25)	298 (+32)
Maximum shear strain in bituminous layer (microstrains)	659	674 (+3)	718 (+9)
σv top of subgrade (kPa)	-39.65	-48.31 (+22)	-56.49 (+42)
εv top of SG (microstrains)	-304.18	-342.87 (+13)	-394.20 (+30)

*The values in parentheses indicate percentage change from case (1) to case (2 and 3)

Table 6. Comparison of pavement responses calculated from FE simulated PET stabilized subgrade model

Pavement responses	Case 1: Standard Axle Loading	Case 2: 1.25 Overloading Factor	Case 3: 1.5 Overloading Factor
δ Surface (mm)	-0.392	-0.451 (+15)	-0.505 (+28)
δ bottom of bituminous layer (mm)	-0.361	-0.425 (+17)	-0.482 (+33)
δ top of subgrade (mm)	-0.092	-0.112 (+21)	-0.129 (+40)
Maximum tensile strain under bituminous layer (microstrains)	220	277 (+26)	293 (+33)
Maximum shear strain in bituminous layer (microstrains)	646	665 (+3)	704 (+9)
σv top of subgrade (kPa)	-37.23	-43.89 (+18)	-51.32 (+38)
εv top of SG (microstrains)	-278.88	-320.14 (+15)	-368.54 (+32)

*The values in parentheses indicate percentage change from case (1) to case (2 and 3)

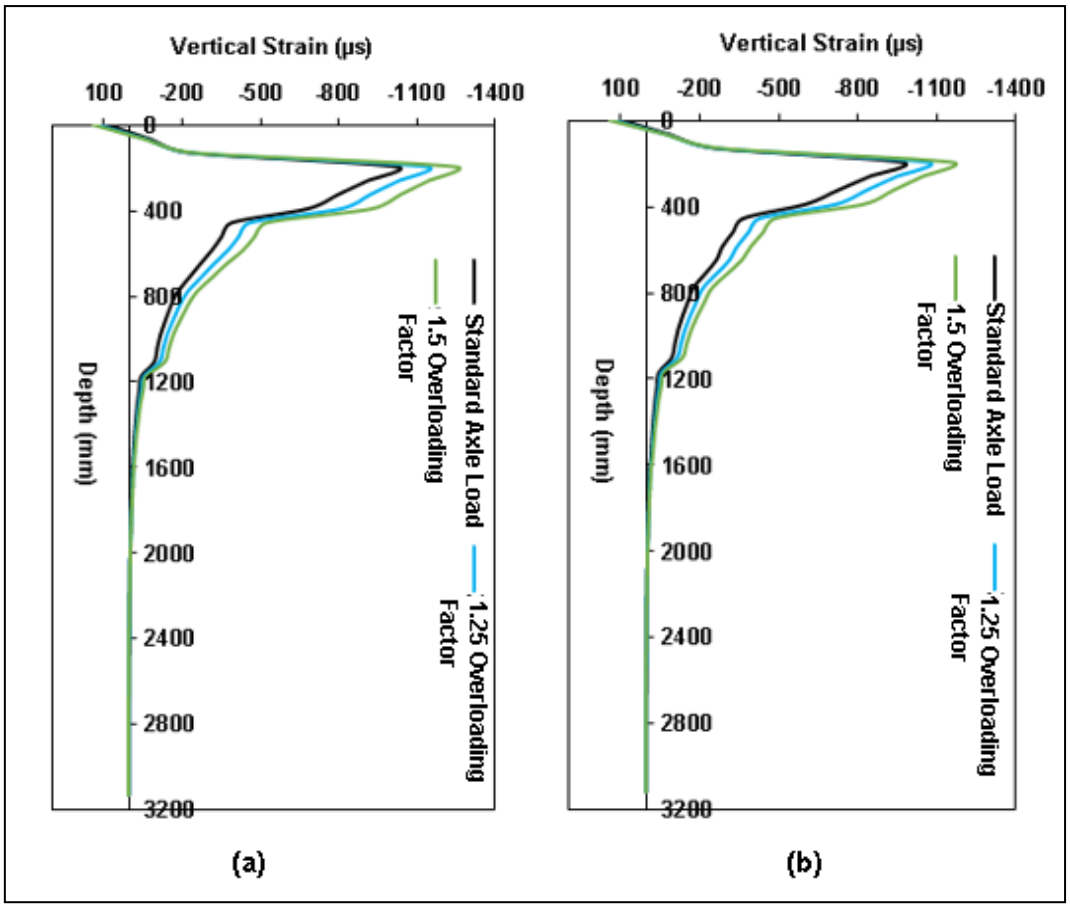

Figure 11. Variation in the vertical rutting strain with depth in (a) Un-stabilized and (b) Stabilized models

Figure 11 (a and b) shows the plot of vertical strain on the pavement under the overloading effect. The improvement in subgrade strength (from 47 MPa to 62 MPa) is attributed to the reduction in compressive strain of 12 percent, which is substantial. This type of improvement in resistance is certainly relevant when the granular layer is also improved in relation to subgrade CBR. From Figure 11, it has been observed that the peak values of the vertical compressive strains at the top of the subgrade are in descending order. When the overloading impact was 1.25 and 1.5 times, the compressive strains at the subgrade increased by 13% and 30%, respectively. Behiry also found that the horizontal tensile and vertical compressive strains increase as the axle load is increased [34]. When standard axle load is applied to pavement 1 and 2, a maximum difference of 25.3 micro strain (304.18-278.88 micro strain) is seen between the subgrade strain values in the two pavements. These findings suggest that the performance of the improved CBR model in terms of strain reduction increases as the elastic modulus of the subgrade is increased, which is consistent with previous findings. Unstabilized subgrade stress ranges from 39.65 to 56.49 kPa, while stabilized subgrade stress ranges from 37.23 to 51.32 kPa. In both cases, increasing axle load increases stress at the top of the subgrade layer. Pavement 2 has fewer compressive stress variations than Pavement 1 due to improved subgrade behaviour.

4.5. Effect of Overloading on Pavement Rutting Life

The vertical strain (ε_v) on the top of the subgrade is used as a fundamental criterion for assessing the rutting life (N_R)of the pavement as per the mechanistic empirical design [35]. The rutting performance of the pavement under axle loads of 40, 50, and 60 kN has been investigated in the present study, considering standard and overloading cases. The relationship involving rutting failure with vertical compressive strain at the top of the subgrade was expressed by equation (3), using the number of load applications in the following equation. In addition to the MoRTH R-56 performance data, the rutting performance equation was established for two separate reliability and performance levels (section 3.6.1 of IRC: 37-2018). The pavement layer thickness used in this investigation was set in accordance with the 50 msa traffic design. As a result, IRC: 37-2018 (section 3.7) guidelines recommend that all major roads use 90% reliability performance equations based on design traffic of 20 msa or greater.

$$N_R = 1.4100 \times 10^{-8} [1/ \varepsilon_v]^{4.5337} \quad (3)$$

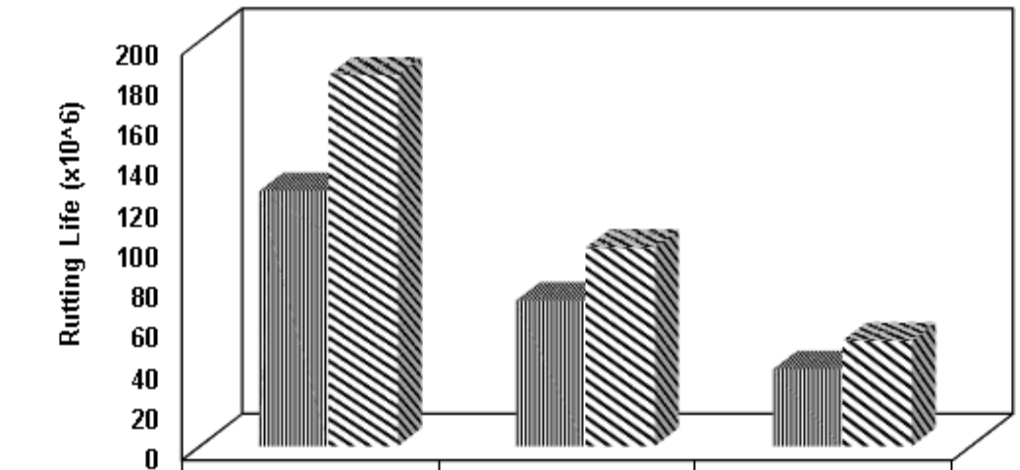

	Standard Loading	25% Overloading	50% Overloading
Pavement 1	126	72	38
Pavement 2	183	98	52

Figure 12. Variation in the rutting performance of un-stabilized and stabilized pavement models

Figure 12 presents the rutting number of cycles before failure for different loading cases to predict the service life of bituminous pavement. This figure shows that the rutting life decreases drastically when the axle load is increased, particularly at axle loads with an overloading factor of 1.5. This analysis resulted in the rutting life measurements of 126, 72, and 38 million for standard, 1.25 overloading, and 1.5 overloading factors, respectively. However, the reduction of the maximum number of repetitions causes rutting by about 1.7 and 3.2 times under the overloading cases. It is undeniable that standard axle loading causes less damage in rutting, but they do significantly more damage when overloading is considered. Comparing the findings of Pavement 2 with a stabilized subgrade layer to the results of the un-stabilized model, it is found that the reduction in rutting life is 31 percent. This demonstrated that the resistance of a pavement to rutting is directly proportional to the strength of the subgrade as well as the amount of overloading increment applied to the pavement surface.

5. Conclusions

Stabilization techniques enhance the engineering parameters of the subgrade soil and generate an upgraded material for construction. This paper has investigated the need for adopting an improved subgrade in flexible pavements with the use of a numerical analysis technique. In view of the expected improvements, this study investigates two important aspects. The first focuses on the improvement of locally available clayey soil stabilized with PET and Terrasil. On the other hand, the effect of a stabilized versus an un-stabilized subgrade model on the evaluation of key responses of pavement structural performance parameters has been investigated. The following conclusions are drawn from the above results and discussions:

- The physical and mechanical characteristics of the soil are improved by the addition of the PET fibre as a fraction of the soil's dry weight. By increasing the proportion of PET fibre, the moisture content and corresponding dry density values decrease.
- The addition of a PET to the subgrade soil increased the CBR by 1.5 times. The improvement in CBR value with ageing treated with 0.1% Terrasil shows an increase in strength. CBR increases by about 18% (7 days of ageing), and 39% (14 days of ageing) for 5% PET.
- The UCS values differ for soil stabilization with PET fibre, as the sequential increment of fibre content does not lead to increased UCS values. However, PET has improved strength parameters, as they show a good increase in cohesion and angle of internal friction.
- With stabilized subgrade, the pavement and component layer thicknesses decrease by 15%, reducing the pavement structure's equivalent mass.
- Pavement characteristics with improved CBR affect the trend of deflection versus axle load. For 1.25 and 1.5 times overloading, the rate of increase is 15% and 30%, respectively. However, as the subgrade modulus increases, the deflection at the surface course, binder course, and top of subgrade is reduced by 3–6%.
- Increased subgrade modulus reduces fatigue and shear strain in the bituminous layer, as well as compressive vertical strain and stress on the subgrade, as shown by comparing critical reactions

of unstabilized and stabilized pavement. Fatigue and shear strain have no significant effect on the stabilized model. When the load is increased by 1.25 and 1.5 times, the fatigue, shear, and rutting strains increase by 26 to 33 percent, 3 to 9 percent, and 15 to 32 percent, respectively.

- Subgrade layers that have been stabilized are better at improving rutting life by 31 percent than those that haven't been stabilized. 25% and 50% overloading cases reduce the number of repetitions required to cause rutting by 1.7 and 3.2 times, respectively.

It may further be stated that the focus of the current study is to investigate the effect of using improved subgrade on the structural behaviour of pavement. The proposed numerical model has considered linear elastic material behaviour for bituminous layers, granular base and sub-base layers, and nonlinear behaviour for subgrade layer. The FE model is validated against available analytical solutions, which are also based on similar assumptions. However, for more realistic modelling of the asphalt concrete layers under overloading, viscoelastic material behaviour needs to be considered in the FE analysis. Efforts for such modification are underway by the authors. Nevertheless, the present study is a step forward to the development of a robust FE model for predicting the structural behaviour of pavements under traffic overloading.

Acknowledgments

The authors would like to thank NIT Durgapur's Department of Civil Engineering for providing the assistance needed to perform the simulations on ANSYS Software. The authors would like to express their gratitude to the Department of Civil Engineering, Dr. B. C. Roy Engineering College, Durgapur for the provision of laboratory facilities to enable the research.

REFERENCES

[1] Sianipar C. P., Dowaki K., "Eco-burden in pavement maintenance: Effects from excess traffic growth and overload," Sustainable Cities and Society, vol. 12, pp. 31-45, 2014. DOI: 10.1016/j.scs.2014.01.002

[2] Savio D., Nivitha M. R., Bindhu B. K., Krishnan J. M., "Overloading analysis of bituminous pavements in India using M-E PDG," Transportation Research Procedia, vol. 17, pp. 607-616, 2016. DOI: 10.1016/j.trpro.2016.11.115

[3] Pais J. C., Amorim S. I., Minhoto M. J., "Impact of traffic overload on road pavement performance," Journal of transportation Engineering, vol. 139, no. 9, pp. 873-879, 2013. DOI: 10.1061/(ASCE)TE.1943-5436.0000571

[4] Rys D., Judycki J., Jaskula P., "Analysis of effect of overloaded vehicles on fatigue life of flexible pavements based on weigh in motion (WIM) data," International Journal of Pavement Engineering, vol. 17, no. 8, pp. 716-726, 2016. DOI: 10.1080/10298436.2015.1019493

[5] Assogba O. C., Tan Y., Sun Z., Lushinga N., Bin Z., "Effect of vehicle speed and overload on dynamic response of semi-rigid base asphalt pavement," Road Materials and Pavement Design, vol. 22, no. 3, pp. 572-602, 2021. DOI: 10.1080/14680629.2019.1614970

[6] Pais J. C., Figueiras H., Pereira P., Kaloush K., "The pavements cost due to traffic overloads," International Journal of Pavement Engineering, vol. 20, no. 12, pp. 1463-1473, 2019. DOI: 10.1080/10298436.2018.1435876

[7] Almeida A., Moreira J. J., Silva J. P., Viteri C. G., "Impact of traffic loads on flexible pavements considering Ecuador's traffic and pavement condition," International Journal of Pavement Engineering, vol. 22, no. 6, pp. 700-707, 2019. DOI: 10.1080/10298436.2019.1640362

[8] Jain A. K., Jha A. K., "Improvement in Subgrade Soils with Marble Dust for Highway Construction: A Comparative Study," Indian Geotechnical Journal, vol. 50, no. 2, pp. 307-317, 2020. DOI: 10.1007/s40098-020-00423-5

[9] Kodicherla S. P. K., Nandyala D. K., "Effect of RBI Grade 81 on strength characteristics of clayey subgrade," International Journal of Geo-Engineering, vol. 8, no. 1, pp. 1-11, 2017. DOI: 10.1186/s40703-017-0061-z

[10] Zhou Z., Chen F., Li C., "Response Factors and Quantitative Characterization for Moisture Equilibria of Subgrade," IOP Conference Series: Earth and Environmental Science, vol. 267, no. 3, pp. 1-6, 2019. DOI: 10.1088/1755-1315/267/3/ 032054

[11] Firoozi A. A., Guney Olgun C., Firoozi A. A., Baghini M. S., "Fundamentals of soil stabilization," International Journal of Geo-Engineering, vol. 8, no. 1, pp. 1-16, 2017. DOI: 10.1186/s40703-017-0064-9

[12] Hassan H. J. A., Rasul J., Samin M., "Effects of plastic waste materials on geotechnical properties of clayey soil," Transportation Infrastructure Geotechnology, vol. 8, no. 3, pp. 390-413, 2021. DOI: 10.1007/s40515-020-00145-4

[13] Amena S., "Utilizing solid plastic wastes in subgrade pavement layers to reduce plastic environmental pollution," Cleaner Engineering and Technology, vol. 7, pp. 100438, 2022. DOI: 10.1016/j.clet.2022.100438

[14] Abukhettala M., Fall M., "Geotechnical characterization of plastic waste materials in pavement subgrade applications," Transportation Geotechnics, vol. 27, pp. 100472, 2021. DOI: 10.1016/j.trgeo.2020.100472

[15] Amena S., "Experimental study on the effect of plastic waste strips and waste brick powder on strength parameters of expansive soils," Heliyon, vol. 7, no.11, pp. 1-6, 2021. DOI: 10.1016/j.heliyon.2021.e08278

[16] Paramkusam B. R., Prasad A., Arya C. S., "A study on CBR behaviour of waste plastic (PET) on stabilised red mud and fly ash," International Journal of Structural and Civil Engineering Research, vol. 2, no. 3, pp. 232-239, 2013. DOI: 10.18178/ijscer

[17] Muntohar A. S., Widianti A., Hartono E., Diana, W.,

"Engineering properties of silty soil stabilized with lime and rice husk ash and reinforced with waste plastic fiber," Journal of Materials in Civil Engineering, vol. 25, no. 9, pp. 1260-1270, 2013. DOI: 10.1061/(ASCE)MT.1943-5533.0000659

[18] Karmakar S., Roy T. K., "Effect of Waste Plastic and Waste Tires Ash on Mechanical Behavior of Bitumen," Journal of Materials in Civil Engineering, vol. 28, no. 6, pp. 04016006- 1-9, 2013. DOI: 10.1061/(ASCE)MT.1943-5533.0001484

[19] Meeravali K., Ruben N., Rangaswamy K., "Stabilization of soft-clay using nanomaterial: Terrasil," Materials Today: Proceedings, vol. 27, no. 2, pp. 1030-1037, 2020. DOI: 10.1016/j.matpr.2020.01.384

[20] Rather M. S., Sharma A., "Stabilization of soil with chemical additives," International Journal of Information Movement, vol. 2, no. VII, pp. 124-130, 2017.

[21] Soundara B., Selvakumar S., Bhuvaneshwari S., "Laboratory study on natural fibre amended fly ash as an expansive soil stabilizer," Geotechnical Engineering Journal of the SEAGS & AGSSEA, vol. 51, no. 4, pp. 1-6, 2020.

[22] Huang Y. H, "Pavement analysis and design." Upper Saddle River, NJ: Pearson Education, 2012.

[23] Sahoo U. C., Reddy K. S., "Effect of nonlinearity in granular layer on critical pavement responses of low volume roads," International Journal of Pavement Research and Technology, vol. 3, no. 6, pp. 320-325, 2010. http://www.ijprt.org.tw/mail web/files/sample/V3N6(5).pdf

[24] Hadi M. N., Bodhinayake B. C., "Non-linear finite element analysis of flexible pavements," Advances in Engineering Software, vol. 34, no. 11-12, pp. 657-662, 2003. DOI: 10.1016/S0965-9978(03)00109-1

[25] Schyns Z. O., Shaver M. P., "Mechanical recycling of packaging plastics: A review," Macromolecular rapid communications, vol. 42, no. 3, pp. 1-27, 2021. DOI: 10.1002/marc.202000415

[26] Banerji A. K., Topdar P., Datta A. K., "Characterization of Stabilized Subgrade on Pavement Performance by means of Finite Element Method," Second ASCE India Conference on Challenges of Resilient and Sustainable Infrastructure Development in Emerging Economies, Kolkata, pp. 1382-1387, March, 2020.

[27] IS 2720 Part 8., "Indian standard methods of test for soil: Determination of MDD & OMC by Heavy Compaction Method," Bureau of Indian Standards, New Delhi, 1983.

[28] IS 2720 Part 16., "Indian standard methods of test for soil: Laboratory determination of CBR," Bureau of Indian Standards, New Delhi, 1987.

[29] IS 2720 Part 10., "Indian standard methods of test for soil: Determination of Unconfined Compressive Strength," Bureau of Indian Standards, New Delhi, 1991.

[30] ASTM D4767-11., "Standard Test Method for Consolidated Undrained Triaxial Compression Test for Cohesive Soils," ASTM Int. West Conshohocken, Pa, 2020.

[31] IRC: 37 2018., "Guidelines for the design of flexible pavements," IRC, New Delhi, India, 2018.

[32] Saad B., Mitri H., Poorooshasb H., "Three-dimensional dynamic analysis of flexible conventional pavement foundation, "Journal of transportation engineering, vol. 131, no. 6, pp. 460-469, 2005. DOI: 10.1061/(ASCE)0733-947X(2005)131:6(460)

[33] Pushpakumara B. H. J., Mendis W. S. W., "Suitability of Rice Husk Ash (RHA) with lime as a soil stabilizer in geotechnical applications," International Journal of Geo-Engineering, vol. 13, no. 1, pp. 1-12, 2022. DOI: 10.1186/s40703-021-00169-w

[34] Behiry A. E. A. E. M., "Fatigue and rutting lives in flexible pavement," Ain Shams Engineering Journal, vol. 3, no. 4, pp. 367-374, 2012. DOI: 10.1016/j.asej.2012.04.008

[35] Mukherjee S., Ghosh P., "Soil behavior and characterization: Effect of improvement in CBR characteristics of soil subgrade on design of bituminous pavements," Indian Geotechnical Journal, vol. 51, no. 3, pp. 567-582, 2021. DOI: 10.1007/s40098-021-00533-8

[36] Kim M., Tutumluer E., Kwon J., "Nonlinear Pavement Foundation Modeling for Three-Dimensional Finite-Element Analysis of Flexible Pavements," International Journal of Geomechanics, vol. 9, no. 5, pp. 195-208, 2009. DOI: 10.1061/(ASCE)1532-3641(2009)9:5(195)

[37] Ghadimi B., Nikraz H., "A comparison of implementation of linear and nonlinear constitutive models in numerical analysis of layered flexible pavement," Road Materials and Pavement Design, vol. 18, no. 3, pp. 550-572, 2013. DOI: 10.1080/14680629.2016.1182055

[38] Rashidi M., Haeri S. M., "Evaluation of behaviors of earth and rockfill dams during construction and initial impounding using instrumentation data and numerical modeling," Journal of Rock Mechanics and Geotechnical Engineering, vol. 9, no. 4, pp. 709-725, 2021. DOI: 10.1016/j.jrmge.2016.12.003